Analyses expérimentales d'écoulement diphasique du réfrigérant dans une machine de froid à absorption de type GAX

Experimental analysis of the refrigerant two-phase flow in an absorption chiller based on GAX cycle

Van Kha PHAM[1,2,3], Nolwenn LE PIERRÈS[1], Hai Trieu PHAN [2,*]

[1] Laboratoire procédés énergie bâtiment (LOCIE) – CNRS, Université Savoie Mont Blanc, Savoie Technolac, 73370 Le Bourget du Lac, France
[2] CEA, LITEN – Université Grenoble Alpes, Campus INES, 73375 Le Bourget du Lac, France
[3] University of Transport and Communications, No 3. Cau Giay Street, Hanoi, Vietnam.
[*](Corresponding author: haitrieu.phan@cea.fr)

Résumé

Cette étude vise à analyser les données expérimentales d'un cycle de réfrigération avec générateur-absorbeur (GAX) ammoniac-eau pour évaluer les différentes conditions de fonctionnement du système. Les résultats permettent de déterminer les conditions thermodynamiques de l'écoulement du fluide frigorigène et d'évaluer les performances de l'évaporateur, qui est présenté comme le composant clé limitant les performances du refroidisseur. Il est démontré que la pureté du fluide frigorigène joue un rôle important dans les conditions d'écoulement diphasique et que l'écart entre les lignes de bulle et de rosée du mélange ammoniac-eau peut conduire à une limitation de la capacité d'évaporation.

Abstract

The main goal of this research is to analyze the experimental data of a ammonia-water Generator-Absorber heat-exchange (GAX) cooling cycle to evaluate the different operating conditions of the system. The results enable to determine the thermodynamic conditions of the refrigerant flow and evaluate the performance of the evaporator, which is shown as the key component limiting the chiller performance. This study demonstrates that the refrigerant purity has a strong role in the two-phase flow conditions and the deviation between the bubble and dew lines of the ammonia-water couple can lead to limitation of the evaporation capacity.

Nomenclature

A	heat transfer area, m^2
Cp	specific heat capacity, kJ/(kg.K)
h	enthalpy, kJ/kg
$\dot{m}$	mass flow rate, kg/h
p	pressure, bar
q_{vap}	Vapour quality, -
$\dot{Q}$	heat flux, kW
x	ammonia mass fraction, -
T	temperature, °C
U	heat transfer coefficient, W/(m^2.K)

Greek symbols

ρ	density, kg/m^3
ε	thermal effectiveness, -
ΔT	temperature difference, K

Index and exponent

A	Absorber
C	Condenser
E	Evaporator
G	Generator
HTF	heat transfer fluid

[*] Auteur correspondant: haitrieu.phan@cea.fr

https://doi.org/10.25855/SFT2025-043

i	inlet	*ref*	refrigerant
l	liquid	*s*	saturated
max	maximum	*sol*	solution
min	minimum	*v*	vapour
o	outlet		

1. Introduction

The International Energy Agency reported the growing demand for cooling over the next three decades as one of the top drivers of global electricity consumption. To cut down the electricity demand and the carbon dioxide emissions, an encouraging alternative to the conventional chillers is the adoption of absorption machines operating with abundant and sustainable heat sources, like solar radiation or industrial waste heat [1]. However, absorption chillers have some disadvantages such as large size, high cost and low efficiency, especially when producing negative temperatures. Several studies have been conducted to improve their performance, including the use of architectures such as double or triple-effect. However, these systems become more complex, leading to more difficult control and higher investment costs. A Generator-Absorber Heat-Exchange (GAX) cycle has a simple architecture like a single-effect cycle, but with higher performance by taking advantage of internal heat recovery. It was first proposed by Altenkrich in 1914 [2]. Due to the temperature difference between the high temperature part of the heat-rejecting absorber and the low temperature part of the heat-absorbing generator ($\Delta T_{overlap}$), the GAX effect allows a part of the heat rejected by the absorption process to be recovered to generate the refrigerant vapor, thereby reducing the required heat from the external heat source supplied at the generator. As the GAX cycles use ammonia-water (NH_3-H_2O) as the working couple, they can operate without crystallization problems [2].

Priedeman et al. [3] conducted an experimental study on an absorption chiller with a cooling capacity of 17.6 kW to produce chilled water at a temperature of 7.2 ℃. The coefficient of performance (*COP*) reached 0.68 compared to a single-effect chiller with a *COP* of only 0.48.

Velázquez and Best [4] analyzed the thermodynamic performance of a 10.6 kW air cooled absorption chiller GAX cycle powered by natural gas and solar energy using air for cooling. When the evaporating temperature was reduced from 4 to -5.5 ℃ at a condensing temperature of 50 ℃, the temperature lift (the temperature difference between the condenser and the evaporator) increases from 46 to 55.5 ℃, but the *COP* decreases from 0.86 to 0.66. This is due to the pressure and temperature of the absorber, decreasing according to the evaporator pressure, thereby reducing the $\Delta T_{overlap}$.

Gómez et al. [5] studied a GAX absorption chiller with cooling power of 10.6 kW using heat source with temperature from 180 to 195 ℃. 55.7% of the heat from internal heat recovery was utilized to create chilled water at 15 ℃ with a *COP* of 0.58.

García-Arellano et al. [6] investigated a dynamic analysis of a shell and tube evaporator with the refrigerant mass flow rate changing from 4 to 8.5 g/s. The chilled water produced had a temperature increased from 13.4 to 18.8 ℃ and the cooling capacity increased from 3.8 to 7.4 kW. A transfer function was found to predict the outlet temperature and cooling capacity, to be used in the control of the GAX cycle.

To our knowledge, there is a lack of information on the operation of absorption chillers GAX cycle to produce negative temperature (down to -20 ℃). Within the framework of the European FriendSHIP project, a prototype of ammonia-water absorption chiller using GAX effect fed by solar heat has been developed to produce cold at -20°C for industrial applications (such as food

preservation and pharmaceuticals) [7]. In the present work, an experimental analysis on this novel architecture is carried out. In the literature, some common assumptions are used, such as at the exits of the condenser and evaporator, the refrigerant is fully condensed or evaporated [8], [9]. However, under the conditions of a cold water exit temperature of -20 °C these conditions are difficult to achieve. To clarify this issue, analysis of the refrigerant flow at the nominal working point of the prototype is carried out. The two-phase condition at the outlet of the evaporator as well as the cooling capacity are evaluated.

2. Experimental data analysis

2.1. Prototype architecture

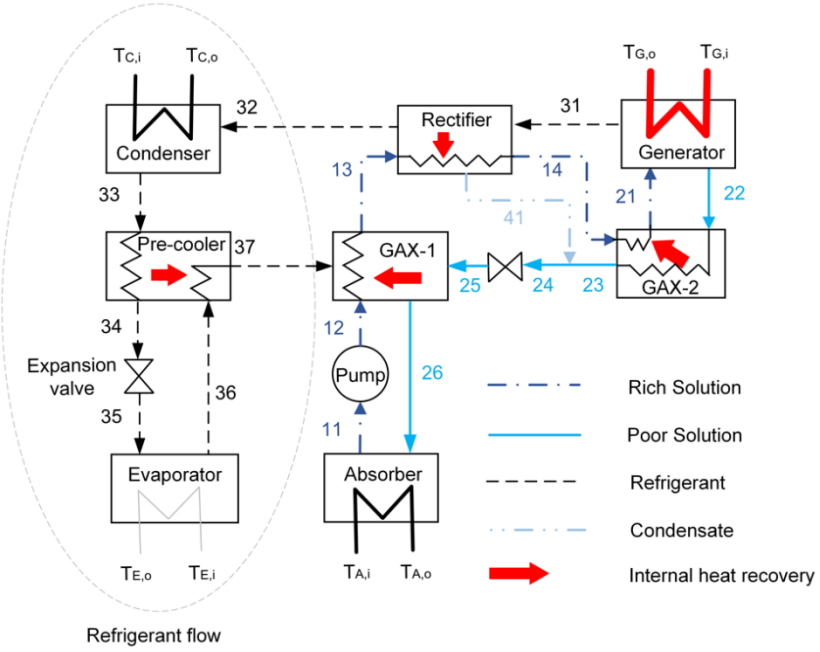

Figure 1: *Schematic of the GAX architecture [7]*

Figure 1 shows the schematic diagram of the FriendSHIP prototype including the main components. Because the system produces chilled water down to -20 °C, the external heat transfer fluid (HTF) of the evaporator is selected as temper -40, the HTF of the remaining components are water. The working principle of this prototype is explained in detail in [7]. Thanks to its innovative architecture based on the GAX effect, a part of the heat rejected by the absorption process is recovered to generate the refrigerant vapor in GAX-1 and GAX-2 (figure 1), thereby reducing the required heat from the external heat source supplied at the generator, and thus improving the performance of the cycle. A rectifier is necessary in the machine, as the volatility of water is close to that of ammonia. Thus, the purity of the vapour exiting the generator at point 32 is high but not strictly equal to 1, as this vapour contains a fraction of water. The refrigerant flow moves from state 32 to state 37, similar to a conventional absorption chiller. The poor solution exits the generator at high temperature in state 22 and is cooled in GAX-2. It then mixes with the condensate from the rectification process at state 41, becoming state 24. From there, it passes through an expansion valve to decrease its pressure and exits at state 25. In this state, it mixes with vapor at state 37 inside GAX-1, leading to the absorption phenomenon which releases heat to the rich solution in the other side of the heat exchanger and transform it from state 12 to state 13. At the outlet of GAX-1, the two-phase solution at state 26 enters the absorber to finish the absorption process by releasing heat to the heat transfer fluid.

2.2. Measurements

To study the limits and effects of different working conditions on the efficiency of the machine, experiments were conducted under 31 different operating steady states in the range shown in Table 1. The prototype is instrumented with 8 Pt100 temperature sensors and 4 flowmeters for the HTF. To determine the internal state parameters of the cycle, 25 thermocouples, 4 pressure gauges, 3 Coriolis flowmeters and 3 liquid level sensors are used.

Table 1: *Experimental campaign matrix for tests carried out on the GAX prototype*

Parameters	Nominal point	Operating range
$T_{G,i}$, ℃	130	120-155
$T_{A,i} = T_{C,i}$, ℃	20	15-25
$T_{E,o}$, ℃	-20	(-20)-(-5)
$\dot{m}_{pump}, kg/h$	170	170-180

2.3. Data processing

To analyze the system performance on the refrigerant flow (as shown in figure 1), parameters that cannot be measured directly will be defined in this section.

By correlation, the mass fraction of the solution and the refrigerant is determined when the temperature and density values are determined:

$$x = f(\rho, T) \tag{1}$$

The thermodynamic properties of the NH_3-H_2O couple were determined using the REFPROP software [10].

The heat flux can be calculated for the HTF as follows:

$$\dot{Q}_{HTF} = \dot{m}_{HTF} \times Cp_{HTF} \times \left|T_{HTF,i} - T_{HTF,O}\right| \tag{2}$$

Additionally, the heat flux can be calculated for the refrigerant side as follows:

$$\dot{Q}_{ref} = \dot{m}_{ref} \times \left|h_{ref,o} - h_{ref,i}\right| \tag{3}$$

Assuming that heat loss to the external environment is neglected, the global heat transfer coefficient of a heat exchanger can be determined by the following formula:

$$U = \frac{\dot{Q}_{HTF}}{A \times \overline{\Delta T}_{ln}} \tag{4}$$

Where: $\overline{\Delta T}_{ln}$ is the log-mean temperature difference, ℃ $\overline{\Delta T}_{ln} = \frac{\Delta T_{max} - \Delta T_{min}}{ln \frac{\Delta T_{max}}{\Delta T_{min}}}$ (5)

To determine the quality of the vapour leaving the evaporator, first the enthalpy at the outlet h_{36} is determined from the energy balance (assuming heat losses are neglected):

$$h_{36} = h_{35} + \frac{\dot{Q}_{E,HTF}}{\dot{m}_{E,ref}} \tag{6}$$

On the other hand, from temperature, pressure and ammonia mass fraction at the exit of the evaporator, we can calculate saturated liquid enthalpy $h_{36,l,sat}$ and saturated vapor enthalpy $h_{36,v,sat}$. The vapour quality q_{vap}, defined as the ratio of the mass flow of the vapour to the total mass flow of the refrigerant, can be calculated according to the following equation:

$$q_{vap} = \frac{h_{36} - h_{36,l,sat}}{h_{36,v,sat} - h_{36,l,sat}} \tag{7}$$

The thermal effectiveness is defined as the ratio of the actual transferred heat to the maximum transferable heat. The thermal effectiveness of evaporator (ε_E) is defined as follows:

$$\varepsilon_E = \frac{\dot{Q}_E}{\dot{Q}_{E,max}} \tag{8}$$

Considering the HFT as the limiting fluid, the maximum heat flux for an ideal evaporator is :

$$\dot{Q}_{E,max} = \dot{Q}_{E,HTF,max} = \dot{m}_{E,HTF} \times Cp_{temper} \times \left(T_{E,i} - T_{35}\right) \tag{9}$$

Where: $Cp_{temper}$is the specific heat capacity of the temper -40 HTF

3. Results and discussion

In order to clearly understand the operating principle of the novel prototype, the nominal point and the effects of the different parameters are investigated.

First, the performance at the nominal point is analyzed. Experimental data shows the prototype's cooling capacity is about 6 kW, with a supply heat of about 16 kW and electricity use of about 0.15 kW. This value of cooling capacity is lower than the design target of 10 kW. Therefore, the analysis of the processes involved in the refrigerant line (points 32 to 37 in Figure 1) is carried out for a better understanding of this deviation.

Table 2 shows the refrigerant experimental state points at different location from the inlet of the condenser (point 32) to the outlet of the pre-cooler (point 37). The condition of the refrigerant at the inlet and outlet of the condenser are shown by states 32 and 33 (figure 1). Point 34 represents the condition of the sub-cooled liquid refrigerant at the exit of the pre-cooler. Point 35 is the outlet of the expansion valve. Unlike the assumption that the enthalpy difference through the throttle valve is ignored, here because the temperature of the refrigerant at the throttle valve (~ -20 °C) is very low compared to the ambient temperature (~ 20 °C) and as the throttle valve is not isolated, there is heat transfer from the ambient to the refrigerant, causing an increase of the enthalpy through this throttle valve. Point 36 represents the exit of the evaporator and the condition of the refrigerant at the exit of the pre-cooler is shown by point 37. The enthalpy of points 36 and 37 are determined from the energy balance equations.

Table 2: *Refrigerant condition at experimental nominal operating conditions*

State points	Pressure (bar)	Temperature (°C)	x (-)	h (kJ/kg)
32	9.86	73.4	0.96	1712
33	9.86	20.3	0.96	392
34	9.86	-19.9	0.96	203
35	1.52	-24.0	0.96	224
36	1.52	-21.0	0.96	1257
37	1.52	3.1	0.96	1446

Figure 2 shows the T-x curves of bubble and dew lines of a NH_3-H_2O mixture at the working measured pressures (p_{32} = 9.86 bar and p_{35} = 1.52 bar). The temperature difference between the dew line and the bubble line at an ammonia mass fraction of 0.96 is huge, around 66 °C with a dew temperature of 44 °C. Since the exchange at the evaporator is limited by the inlet temperature of the HTF ($T_{E,i}$ = -17 °C), the condition for a complete evaporation of the

refrigerant can never be reached, therefore, the refrigerant exits the evaporator in two-phase condition.

As shown in Figure 3, the refrigerant continues to be evaporated in the pre-cooler (36 to 37). However, leaving the pre-cooler, the point 37 of the refrigerant is still in two-phase condition since the point 37 cannot reach the dew point line. The temperature of point 37 is limited by the pre-cooler efficiency as well as the temperature of point 33. The return of liquid refrigerant to the absorber is an efficiency loss for the cycle.

The above analysis shows that the evaporator is undersized and is the key component which limits the cooling capacity of the chiller. In order to identify ways to improve its design, analysis of the evaporator performance is described in the following paragraphs.

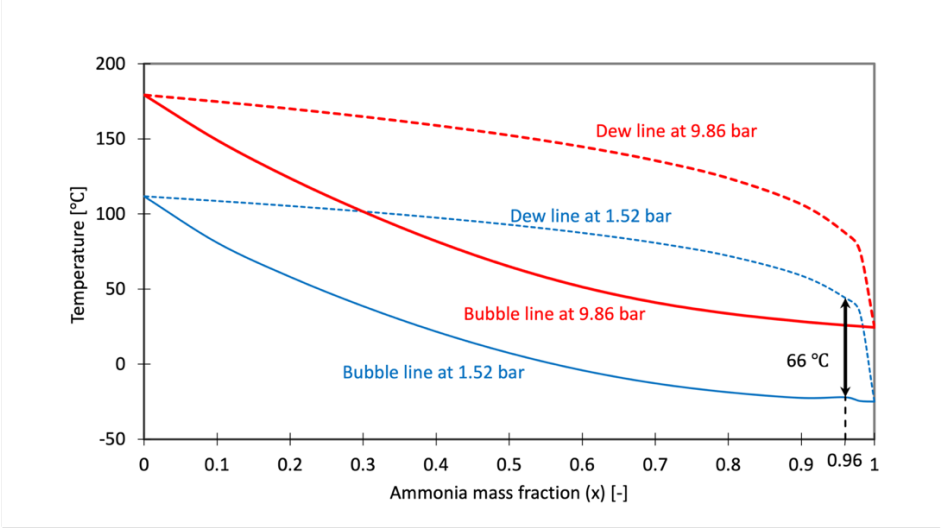

Figure 2: *T-x diagram of refrigerant at nominal point*

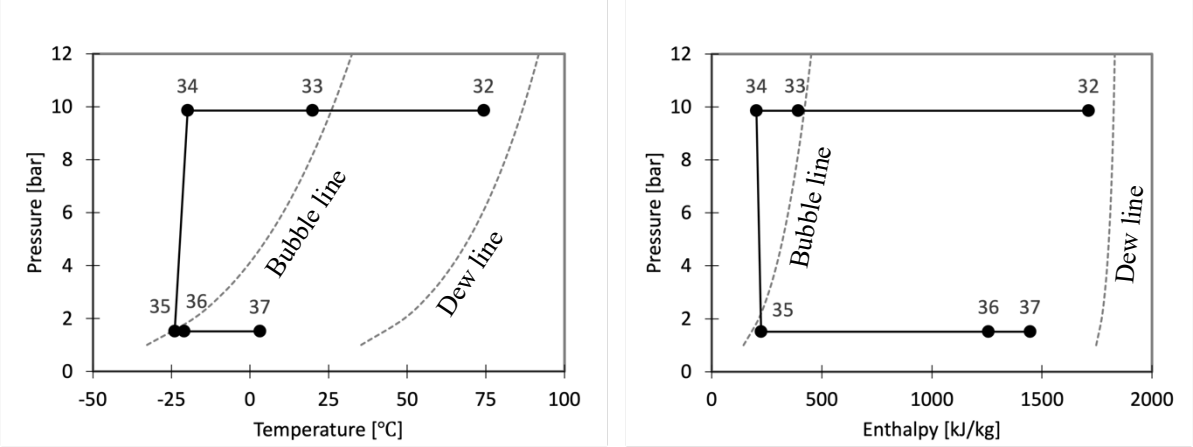

a) P-T diagram b) P-h diagram

Figure 3: *P-T and P-h diagrams of the refrigerant at x = 0.96*

Figure 4 illustrates the effect of refrigerant mass flow rate $\dot{m}_{ref}$, which varies with the evaporator temperature ($T_{E,o}$ from -20 °C to -5 °C), on the global heat transfer coefficient U_E when $T_{G,i}$ from 120 to 150 °C. When $\dot{m}_{ref}$ changes from 20 to 36 kg/h, U_E increases from 2300 to 2900 W/(m^2.K). The thermal effectiveness of the evaporator ε_E increases linearly with U_E and reaches a maximum value of 0.46 as shown in Figure 5. This value of ε_E is quite low compared to the selected design and simulation conditions (typically 0.80).

Figure 6 shows the experimental value of the vapour mass flow rate of refrigerant $\dot{m}_{ref,vapour}$ and the vapour quality (q_{vap}) at point 36 as functions of $\dot{m}_{ref}$. The vapour quality

remains nearly constant (around 0.75 to 0.80), leading to a linear increase of $\dot{m}_{ref,vapour}$ exit of the evaporator from 15 to 27 kg/h.

Figure 7 illustrates the effect of the change in the amount of vapor produced by the evaporator with the cooling capacity. At the point where $\dot{m}_{ref,vapour}$ is about 18.5 kg/h in Figure 7, this stability is not good compared to other conditions because of the very low inlet temperature the generator (120 °C). In some working conditions ($T_{G,i}$ from 120 to 150 °C) the cooling capacity increases to reach 10 kW thanks to the increase in the amount of vapor produced.

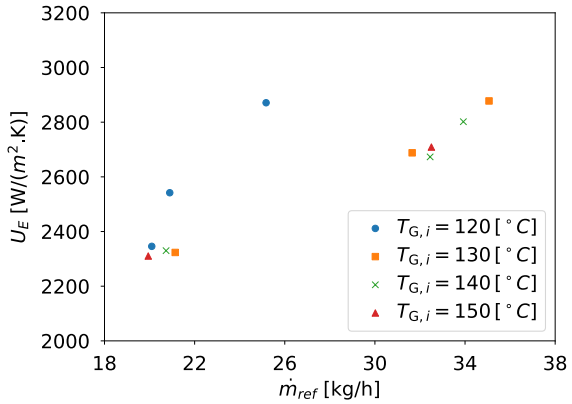

Figure 4: *Evaluation of the relationship between U_E and $\dot{m}_{ref}$ with varying $T_{G,i}$ at $T_{A,i}$ = 20 °C*

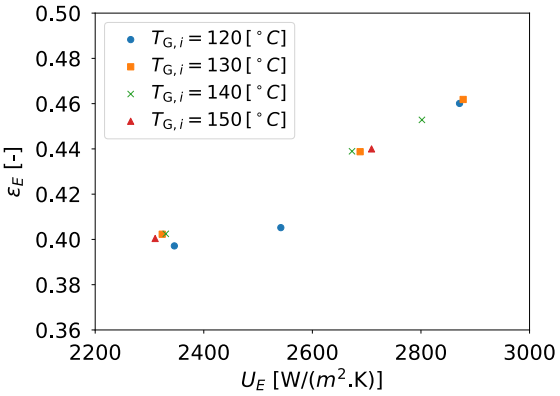

Figure 5: *Evaluation of the relationship between ε_E and U_E with varying $T_{G,i}$ at $T_{A,i}$ = 20 °C*

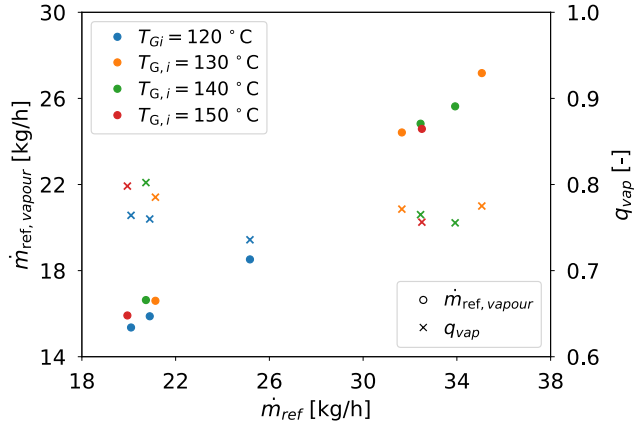

Figure 6*: Evaluation of the relationship between $\dot{m}_{ref,vapour}$, q_{vap} and $\dot{m}_{ref}$ with varying $T_{G,i}$ at $T_{A,i}$ = 20 °C*

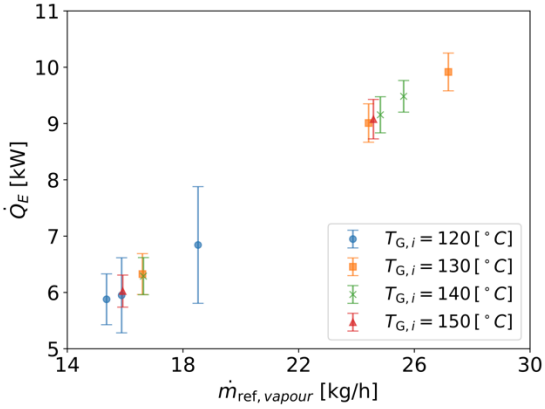

Figure 7*: Evaluation of the relationship between $\dot{Q}_E$ and $\dot{m}_{ref,vapour}$ with varying $T_{G,i}$ at $T_{A,i}$ = 20 °C*

This analysis shows that the impure refrigerant with an ammonia mass fraction of 0.96 has a strong impact on the thermodynamic conditions of the refrigerant in the evaporator, leading to strong limitation in term of the evaporation capacity. Therefore, to improve the chiller performance, it is important to focus not only on the evaporator size but also on the purity of the refrigerant generated, and as a consequence on the desorber design and dimensioning.

4. Conclusion

In this paper, the experimental data of a novel GAX absorption chiller were analyzed in order to identify two-phase conditions of the refrigerant flow. This analysis gives insight to explain why the measured cooling power (6 kW) is lower than the target power (10 kW). The low

thermal effectiveness of the evaporator (<0.46) is related to not only its geometry but also to the imposed thermodynamic conditions. The impure refrigerant with an ammonia mass fraction of 0.96 is the main factor that limits the evaporation capacity by a huge difference between the bubble and dew temperatures for that mixture. Thanks to this work, a way to improve the chiller performance was identified as a change of not only the evaporator sizing but also of the desorption process in order to improve the refrigerant quality.

References

[1] D. N. Nkwetta and J. Sandercock, A state-of-the-art review of solar air-conditioning systems, *Renewable and Sustainable Energy Reviews*, vol. 60, pp. 1351–1366, Jul. 2016, doi: 10.1016/j.rser.2016.03.010.

[2] K. E. Herold, R. Radermacher, and A. K. Sanford, *Absorption Chillers and Heat Pumps*, Second Edition. CRC Press, 2016.

[3] D. K. Priedeman, M. Garrabrant, J. A. Mathias, R. Stout, and R. N. Christensen, Performance of a Residential-Sized GAX Absorption Chiller, *Journal of Energy Resources Technology*, 2001, doi: doi.org/10.1115/1.1385519.

[4] N. Velázquez and R. Best, Methodology for the energy analysis of an air cooled GAX absorption heat pump operated by natural gas and solar energy, *Applied Thermal Engineering*, vol. 22, no. 10, pp. 1089–1103, Jul. 2002, doi: 10.1016/S1359-4311(02)00028-5.

[5] V. H. Gómez, A. Vidal, R. Best, O. García-Valladares, and N. Velázquez, Theoretical and experimental evaluation of an indirect-fired GAX cycle cooling system, *Applied Thermal Engineering*, vol. 28, no. 8–9, pp. 975–987, Jun. 2008, doi: 10.1016/j.applthermaleng.2007.06.027.

[6] C. García-Arellano, O. García-Valladares, and V. H. Gómez, Experimental analysis of a transfer function for the transient response of an evaporator in an absorption refrigeration GAX system, *Applied Thermal Engineering*, vol. 30, no. 14–15, pp. 2026–2033, Oct. 2010, doi: 10.1016/j.applthermaleng.2010.05.008.

[7] H. Demasles, A. Muller, and H. T. Phan, Development of ammonia-water absorption chillers for negative cooling in industrial solar systems, presented at the 26th IIR International Congress of Refrigeration, Paris , France, Aug. 2023. doi: 10.18462/iir.icr.2023.0054.

[8] A. S. Mehr, M. Yari, S. M. S. Mahmoudi, and A. Soroureddin, A comparative study on the GAX based absorption refrigeration systems: SGAX, GAXH and GAX-E, *Applied Thermal Engineering*, vol. 44, pp. 29–38, Nov. 2012, doi: 10.1016/j.applthermaleng.2012.03.033.

[9] A. S. Mehr, V. Zare, and S. M. S. Mahmoudi, Standard GAX versus hybrid GAX absorption refrigeration cycle: From the view point of thermoeconomics, *Energy Conversion and Management*, vol. 76, pp. 68–82, Dec. 2013, doi: 10.1016/j.enconman.2013.07.016.

[10] E. H. Lemon, I. H. Bell, M. L. Huber, and M. O. McLinden, *NIST Standard Reference Database 23: Reference Fluid Thermodynamic and Transport Properties-REFPROP, Version 10.0, National Institute of Standards and Technology*. (2018). National Institute of Standards and Technology, Gaithersburg. [Online]. Available: https://www.nist.gov/srd/refprop

Acknowledgements

Van Kha Pham received funding from the Vietnam Government Scholarship (Project 89, decision n° 2314/QĐ-BGDĐT dated 11/08/2023). The authors would like to express their gratitude to the French Alternative Energies and Atomic Energy Commission for the funding of this research (Contract n° C46726). We would like to thank the members of the European FriendSHIP project for their valuable research contributions and providing us with the experimental data used in this study.